Relatively Selective Production of the Simplest Criegee Intermediate in a CH 4 /O 2 Electric Discharge: Kinetic Analysis of a Plausible Mechanism

ARTICLE *in* THE JOURNAL OF PHYSICAL CHEMISTRY A · NOVEMBER 2014

Impact Factor: 2.69 · DOI: 10.1021/jp510554g · Source: PubMed

3 AUTHORS, INCLUDING:

Thanh Lam Nguyen
University of Texas at Austin
72 PUBLICATIONS **1,382** CITATIONS
SEE PROFILE

John F Stanton
University of Texas at El Paso
251 PUBLICATIONS **10,463** CITATIONS
SEE PROFILE

THE JOURNAL OF PHYSICAL CHEMISTRY A

Article

pubs.acs.org/JPCA

Relatively Selective Production of the Simplest Criegee Intermediate in a CH_4/O_2 Electric Discharge: Kinetic Analysis of a Plausible Mechanism

Thanh Lam Nguyen,[†] Michael C. McCarthy,[‡] and John F. Stanton*,[†]

[†]Department of Chemistry, The University of Texas at Austin, Mail Stop A5300, Austin, Texas 78712-0165, United States

[‡]Harvard-Smithsonian Center for Astrophysics, 60 Garden Street, Cambridge, Massachusetts 02138, United States

Supporting Information

ABSTRACT: High -accuracy coupled cluster methods in combination with microcanonical semiclassical transition state theory are used to investigate a plausible formation mechanism of the simplest Criegee intermediate in a CH_4/O_2 discharge experiment. Our results suggest that the Criegee intermediate is produced in a three-step process: (i) production of methyl radical by cleavage of a C−H bond of CH_4; (ii) association of methyl radical with molecular oxygen to form a vibrationally excited methyl peroxy, which is in a rapid microequilibrium with the reactants; and finally, (iii) H-abstraction of CH_3OO by O_2, which results in the formation of cool CH_2OO, which has insufficient internal energy to rearrange to dioxirane.

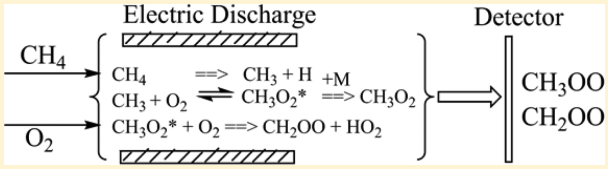

INTRODUCTION

Long celebrated in the subject of organic chemistry has been the so-called Criegee intermediate (carbonyl oxide), a compound formed during the ozonolysis of alkenes, e.g.,

$$O_3 + H_2C{=}CH_2 \rightarrow CH_2O + H_2C{=}O{-}O$$

which was first postulated in 1949.[1,2] Although the existence of the Criegee intermediate has been confirmed through indirect (trapping) methods,[3,4] direct observation of this seemingly elusive species did not occur until quite recently.[5−7] In 2008, the simplest Criegee species $H_2C{=}O{-}O$ was observed with tunable synchrotron photoionization mass spectroscopy by Taatjes and co-workers.[5,6] These workers produced the intermediate by photolysis of CH_2I_2 in the presence of molecular oxygen, conditions that apparently serve to generate $H_2C{=}O{-}O$ with reasonable efficiency. Subsequent spectroscopic studies using the same basic production method occurred soon thereafter, and now include studies using microwave and infrared spectroscopies[7,8] and electronic spectroscopy.[9]

Recently, McCarthy et al.[10] succeeded in generating $H_2C{=}O{-}O$ in an electrical discharge, starting from two simple precursors: methane and molecular oxygen. Unlike production of this molecule from methylene iodide, both of these compounds are common in the atmosphere, and the generation of the Criegee intermediate in this experiment suggests that it might be formed in the vicinity of atmospheric lightning strikes, which occur approximately 1.4×10^9 times annually.[11,12] Surprisingly, the production of $H_2C{=}O{-}O$ in the CH_4/O_2 discharge appears to be fairly selective: although this molecule is the least stable isomer of CH_2O_2, very little evidence for the overwhelmingly more stable formic acid is found in the microwave spectrum. In addition, both the cyclic compound dioxirane and dihydroxycarbene—both of these isomers having known microwave spectra—were conspicuously absent in the same discharge.

For these reasons, $H_2C{=}O{-}O$ production in the methane/oxygen discharge warrants further study to better understand the underlying formation mechanism. Since an electronic discharge is a complicated environment, a standard kinetics analysis of the reaction system is not possible, and any results of such a study must remain largely qualitative and somewhat speculative in nature. In this short paper, we document a plausible scenario by which relatively clean generation of stabilized and relatively cold $H_2C{=}O{-}O$ might be achieved in a CH_4/O_2 discharge. An exploratory microcanonical analysis of the chemical kinetics is also considered, and suggests that relatively selective generation of $H_2C{=}O{-}O$ is indeed possible at energies typically accessible in a discharge experiment.

QUANTUM CHEMICAL CALCULATION

For small chemical species, which have three (or less than three) heavy atoms as displayed in Figure 1, the HEAT-345(Q) protocol is a practical and highly accurate means for determining energies.[13−15] It is well established that this level of theory can provide an accurate relative energy, within 0.25 kcal/mol (1 kJ/mol), for stationary points whose electronic

Special Issue: 100 Years of Combustion Kinetics at Argonne: A Festschrift for Lawrence B. Harding, Joe V. Michael, and Albert F. Wagner

Received: October 20, 2014
Revised: November 16, 2014

   dx.doi.org/10.1021/jp510554g | J. Phys. Chem. A XXXX, XXX, XXX−XXX

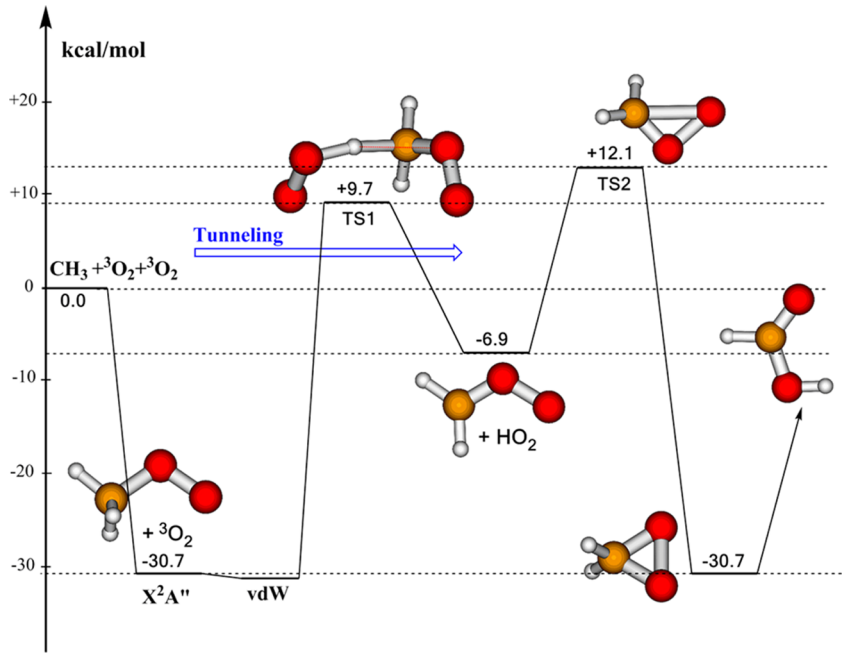

Figure 1. Schematic reaction energy profile for forming the simplest Criegee intermediate in the CH_4/O_2 electric discharge experiment, constructed using the mHEAT-345(Q) method.

wave functions are dominated by a single determinant Hartree−Fock reference function.[13−15] However, for molecules such as TS1 in Figure 1—which has five heavy atoms and is an open-shell species—HEAT-345(Q) calculations are very demanding and other schemes become desirable alternatives. Therefore, a less accurate method that is a modification of the original HEAT-345(Q) protocol, designated here as mHEAT-345(Q), will be applied in this work. In this simplified protocol, stationary points on the lowest-lying doublet electronic state potential energy surface for reaction of CH_3 and O_2 (as presented in Figure 1) to produce the $H_2C{=}O{-}O$ molecule are optimized using coupled-cluster with single, double, and noniterative triple excitations (CCSD(T)) in combination with the atomic natural orbital basis set of Taylor and Almlöf[16,17] designated as ANO1.[18] Harmonic frequency analysis is subsequently done to characterize stationary points located: all $3N-6$ real frequencies for a minimum and only one imaginary frequency for a transition structure (TS). Anharmonic force fields are also computed using the same CCSD(T) method, but with a smaller basis set (ANO0)[18] to obtain anharmonic constants. The zero-point vibrational energy (ZPE) is then calculated with second-order vibrational perturbation theory (VPT2)[19] using the harmonic CCSD(T)/ANO1 and anharmonic CCSD(T)/ANO0 force fields. The frozen-core approximation is used in all such calculations. A complete documentation of mHEAT-345(Q) is as follows:

i. Molecular geometries are optimized with CCSD(T)/ANO1 level of theory in the frozen-core (FC) approximation.
ii. ZPEs are computed using second-order vibrational perturbation theory (VPT2). The FC−CCSD(T)/ANO1 harmonic and FC−CCSD(T)/ANO0 anharmonic force fields are used.
iii. SCF-HF energies are calculated using the correlation consistent basis sets cc-pVXZ (with X = 3(T), 4(Q), and 5).[20] These three energies are then extrapolated to the complete basis set limit in order to obtain the SCF-HF energy.[21]

$$E_{\mathrm{HF}}^{X} = E_{\mathrm{HF}}^{\infty} + a\exp(-bX)$$

iv. CCSD(T) correlation energies are calculated using the basis sets cc-pVXZ (with $X = 4$ (Q) and 5). The frozen-core (FC) CCSD(T) correlation energy extrapolated to the complete basis set limit is then obtained.[22]

$$\Delta E_{\mathrm{CCSD(T)}}^{X} = \Delta E_{\mathrm{CCSD(T)}}^{\infty} + aX^{-3}$$

v. Core−valence correction energies are calculated as the difference in energy between (all electron) AE-CCSD(T)/cc-pCVTZ and FC−CCSD(T)/cc-pVTZ levels of theory.

$$\Delta E_{\mathrm{Core}} = \Delta E_{\text{cc-pCVTZ}} - \Delta E_{\text{cc-pVTZ}}$$

vi. Triple excitation effects that are not included in the CCSD(T) treatment of correlation are estimated as the difference in energy between FC−CCSDT/cc-pVTZ and FC−CCSD(T)/cc-pVTZ levels of theory.

$$\Delta E_{\mathrm{T-(T)}} = \Delta E_{\mathrm{CCSDT}} - \Delta E_{\mathrm{CCSD(T)}}$$

vii. Noniterative quadruple excitation corrections are obtained as a difference in energy between FC−CCSDT(Q)/cc-pVDZ and FC−CCSDT/cc-pVDZ levels of theory.

$$\Delta E_{\mathrm{(Q)-T}} = \Delta E_{\mathrm{CCSDT(Q)}} - \Delta E_{\mathrm{CCSDT}}$$

viii. The diagonal Born−Oppenheimer correction (DBOC) is calculated using SCF-HF/aug-cc-pVTZ level of theory. RHF and ROHF methods are used for closed- and open-shell systems, respectively.

dx.doi.org/10.1021/jp510554g | J. Phys. Chem. A XXXX, XXX, XXX−XXX

ix. Spin−orbit corrections are taken from experiment whenever they are available (however, no molecules studied in this research are in degenerate electronic states, so none exhibits a first-order SO effect, but this is included for the purpose of completing the description).
x. Scalar relativistic effects including one- and two-electron Darwin, and mass-velocity terms are calculated using SCF-HF/aug-cc-pCVTZ level of theory.

The total energy of mHEAT method can be then expressed in the usual manner:[13]

$$E_{\mathrm{mHEAT}} = E_{\mathrm{HF}}^{\infty} + \Delta E_{\mathrm{CCSD(T)}}^{\infty} + \Delta E_{\mathrm{Core}} + \Delta E_{\mathrm{T-(T)}} + \Delta E_{\mathrm{(Q)-T}} + \Delta E_{\mathrm{REL}} + \Delta E_{\mathrm{ZPE}} + \Delta E_{\mathrm{DBOC}} + \Delta E_{\mathrm{SO}}$$

with the understanding that each contribution is defined as above.

As an initial and simple test of mHEAT, we calculated the binding energy of methylperoxy radical, an important intermediate that is formed by combination of methyl radical with triplet O_2, using mHEAT and HEAT-345(Q) methods. The results presented in Table 1 show that mHEAT gives a value of 30.7 kcal/mol, which is in excellent agreement with an ATcT value of 30.61 ± 0.24 kcal/mol[23−26] as well as 30.4 kcal/mol obtained with HEAT-345(Q) protocol.[13−15] It is therefore plausible to expect that the mHEAT method, which can be used for medium-sized reaction systems, may provide an energy for stable chemical species that is sufficiently accurate to be suitable for largely qualitative studies such as that reported in this research.

Table 1. Contributions of Energies (kcal/mol) (Relative to $CH_3 + 2O_2$) of Various Terms to Barrier Height and Binding Energy of CH_3OO Calculated Using a Modified HEAT Method (See Text)

term	barrier height	$CH_3OO(X^2A'') + O_2$
Δ_{SCF}	46.80	−15.14
$\Delta_{\mathrm{CCSD(T)}}$	−36.72	−21.67
$\Delta_{\mathrm{T-(T)}}$	−2.24	−0.19
$\Delta_{\mathrm{(Q)-T}}$	−1.44	0.24
Δ_{ZPE}	2.75	5.90
Δ_{Core}	0.29	0.00
Δ_{DBOC}	0.07	−0.02
Δ_{Scalar}	0.15	0.12
Δ_{SO}	0.00	0.00
total	9.66	−30.75
		(HEAT: −30.40)[a]
		[ATcT: −30.61 ± 0.24][b]

[a]Obtained with HEAT-345(Q) method. [b]Taken from ATcT.[23−26]

The CFOUR quantum chemistry program[27] was used for all of the calculations reported here except that of the CCSDT(Q) energy, which used the MRCC code,[28] as interfaced with CFOUR.

CHEMICAL REACTION MECHANISM

In the original study,[10] a mixture of CH_4 and O_2 gases was passed through an electric discharge and the simplest Criegee, CH_2═O−O, is apparently produced with high selectivity. Here, we propose a possible reaction mechanism (as shown in Figure 1) that leads to formation of "cool" CH_2═O−O, as is required in light of the absence of other CH_2O_2 isomers, particularly the dioxirane molecule, which is separated from the less stable H_2C═O−O by a barrier of only 19.0 kcal/mol. The first step in this mechanism is production of methyl radicals from CH_4 either by breaking a C−H bond or hydrogen abstraction by "hot" O_2, processes that almost certainly take place in the discharge. Once methyl radical is formed, it can rapidly combine with O_2, which is present in excess relative to CH_3, to form vibrationally excited methylperoxy radical (CH_3OO). This species has an excess internal energy of (at least) 30.7 kcal/mol, which is the C−O bond energy calculated, as mentioned in the last section with mHEAT-345(Q) (30.4 with HEAT, see Table 1). Further dissociation of "hot" nascent methylperoxy radicals is not favored because this process requires additional energy still (at least 58 kcal/mol).[29] Instead, CH_3OO—which is observed as one of the discharge products—will rapidly redissociate to CH_3 plus O_2 as soon as it is formed, therefore resulting in rapid establishment of the microcanonical equilibrium $CH_3 + O_2 \leftrightharpoons CH_3OO^*$ (here, CH_3OO^* with an asterisk represents "hot" CH_3OO species that are in vibrationally excited states). "Hot" methylperoxy radical could lose some of its internal energy by collision with a third body (e.g., O_2, CH_4 or—more likely as it is present in great excess of either oxygen or methane—the inert buffer gas in the experiment). Detection of CH_3OO indicates that some fraction of these energetic species are collisionally stabilized on the time scale of the expansion, owing to the large number of collisions.[10]

Competing with both dissociation and collisional relaxation, however, is the reaction of hot CH_3OO^* with another O_2 molecule, which can promptly extract a hydrogen atom to form CH_2═O−O plus HO_2. This reaction path takes place via TS1 and faces a substantial barrier, calculated to be 40.4 kcal/mol (which is 9.7 kcal/mol above the asymptotic energy of the initial reactants, $CH_3 + 2O_2$). Contributions of various terms to the calculated barrier height are displayed in Table 1. As can be seen in Table 1, the simple (SCF-HF) method gives a typically horrendous estimate of the barrier height, which is reduced by 36.7 kcal/mol at the CCSD(T) level. The next most important contribution is the ZPE with a contribution of +2.8 kcal/mol. Both triple and quadruple excitations also play important roles and have the same sign, acting together to reduce the barrier by 3.7 kcal/mol. Other contributions are small. It is important to note that this barrier is calculated based on the unrestricted HF reference (as is always the case with HEAT-based calculations), whose wave function in this case has a high spin-contamination of about $\langle S^2 \rangle = 1.76$. This problem is due to interference of quartet (and higher spin multiplicity) electronic states that obviously arise from the interaction of a triplet electronic state of O_2 with a doublet electronic state of CH_3OO. When the restricted open-shell HF reference is used, the calculated barrier is reduced by 1.0 to 39.4 kcal/mol. The fact that the high-level coupled-cluster calculation of the barrier height is relatively insensitive to the quite serious spin-contamination of the UHF reference is due to the presence of the (exponential) single excitation operator in the coupled cluster wave function, which tends to ameliorate effects due to orbital choice and is well-known.[30] Adopting an average of these two values, we obtain a barrier of 39.9 kcal/mol (or 9.2 kcal/mol above $CH_3 + 2O_2$) with an estimated error bar of about ±2 kcal/mol, a value that will be used in the following section in a chemical kinetic analysis.

dx.doi.org/10.1021/jp510554g | J. Phys. Chem. A XXXX, XXX, XXX−XXX

Although the barrier for the H-abstraction step is quite high, TS1 is only about 9 to 10 kcal/mol above the asymptotic energy level of the reactants. Consequently, the formation of the Criegee intermediate by the H-abstraction path via TS1 is certainly possible in the discharge, given the likely presence of vibrationally excited CH_3* and O_2*. Thus, a portion of this required energy can be donated to nascent CH_3OO* that already has an internal energy of 30.7 kcal/mol. This process will lead to enhanced formation of CH_2=O−O. At this point, there are four possible outcomes, all subject to the initial internal energy of the CH_3OO* + O_2 reaction system: (1) Criegee formation cannot occur (by any mechanism) if the internal energy of CH_3OO* and O_2 is below that of the Criegee minimum; (2) if the internal energy of CH_3OO* and O_2 is between that of Criegee and TS1, nascent Criegee can be formed by quantum mechanical tunneling through TS1; (3) if the internal energy of CH_3OO* and O_2 is slightly higher than TS1, nascent Criegee when formed may be cool because a part of the total internal energy may be lost to translational degrees of freedom and to HO_2 after passing TS1; and finally, (4) Criegee produced will be highly vibrationally excited if the internal energy of the reactants is much higher than TS1. Hot Criegee with sufficient internal energy can then ring-close via TS2 (overcoming a barrier of 19.0 kcal/mol) leading to dioxirane, which will then quickly isomerize to formic acid and subsequently give various products such as H_2 + CO_2, H_2O + CO, HO + HCO, and H + HOCO. A similar reaction mechanism starting with hot Criegee produced by O_3 + C_2H_4 reaction was reported in literature earlier,[31−33] and is an ongoing project in our laboratories. In the discharge experiment, however, at least some Criegee must be formed that is relatively "cold". Some fraction of hot Criegee could conceivably be stabilized by collisions with the bath gas in the nozzle source, but this outcome seems unlikely given the apparent absence of other much more stable products such as formic acid.

It should be noted that excited states of O_2 may be present in the discharge. The excited singlet $^1\Delta$ state of O_2 lies 22.6 kcal/mol[34] above ground state triplet O_2. The association of singlet O_2 with CH_3, however, will correlate to the first excited state $^2A'$ of CH_3OO (not shown in Figure 1, see Table S1), which is about 21 kcal/mol above the ground state X^2A'' of CH_3OO. Moreover, the first excited state $^2A'$ of CH_3OO does not correlate to the products CH_2=O−O + HO_2. Nevertheless, it could be that $CH_3OO(^2A')$ can undergo internal conversion to the ground state, which would likely result in vibrationally hot CH_3OO* in the electronic ground state. As a result, "hot" Criegee will then be produced and will consequently not survive long enough for detection.

CHEMICAL KINETICS ANALYSIS

To investigate the plausibility of the above-mentioned reaction mechanism (see Figure 1), we carried out calculations of the microcanonical rate constant as a function of internal energy for the CH_3OO* + $O_2 \underset{\text{fast}}{\longleftrightarrow}$ vdW* $\underset{\text{slow}}{\longrightarrow}$ CH_2=O−O + HO_2 reaction path in the overall reaction scheme, $CH_3 + 2O_2 \underset{\text{fast}}{\longleftrightarrow}$ CH_3OO* + $O_2 \underset{\text{fast}}{\longleftrightarrow}$ vdW* $\underset{\text{slow}}{\longrightarrow}$ TS1 → CH_2=O−O + HO_2, using the microcanonical version of semiclassical transition state theory (SCTST)[35−39] (also see Schemes 1 and 2). It should be mentioned that only the portion of CH_3OO* in vibrationally excited states can react with O_2, whereas the fraction that is collisionally stabilized is chemically inactive.

Scheme 1. Fast Equilibrium between CH_3 + O_2 and CH_3OO

$$CH_3 + O_2 \underset{}{\overset{\text{Fast}}{\rightleftharpoons}} CH_3OO^* \xrightarrow{+M} CH_3OO$$

Scheme 2. Formation of Criegee from the CH_3OO* + O_2 Reaction

$$CH_3OO^* + O_2 \underset{k_{-1}(E,J)}{\overset{k_1(E,J)\ \text{Fast}}{\rightleftharpoons}} \text{vdW}^* \xrightarrow[k_2(E,J)]{\text{Slow}} \text{TS1} \longrightarrow CH_2OO + HO_2$$

According to Scheme 2, the microcanonical rate constant, $k(E,J)$, for the formation of Criegee from the H-abstraction reaction of vibrationally excited CH_3OO* by O_2 is calculated as eq 1:

$$k(E,J) = K_C(E,J) \times k_2(E,J) \tag{1}$$

$$K_C(E,J) = \frac{k_1(E,J)}{k_{-1}(E,J)} = \frac{\rho(E,J)_{\text{vdW}}}{\rho(E,J)_{\text{Re}}} \tag{2}$$

$$k_2(E,J) = \frac{\sigma}{h} \times \frac{G(E,J)_{\text{TS1}}}{\rho(E,J)_{\text{vdW}}} \tag{3}$$

where K_C is the microcanonical equilibrium constant. k_2 is the microcanonical rate constant for the vdW* → CH_2=O−O + HO_2 step, which is calculated using SCTST. In this regard, SCTST is like RRKM theory,[36] but it includes fully coupled anharmonic vibrations (treated with VPT2) and implicitly includes effects of multidimensional quantum tunneling effects in the sum and density of states. Substituting eqs 2 and 3 into 1, the microcanonical rate constant for the Criegee formation can finally be expressed as eq 4:

$$k(E,J) = \frac{\sigma}{h} \times \frac{G(E,J)_{\text{TS1}}}{\rho(E,J)_{\text{Re}}} \tag{4}$$

where σ is the reaction path degeneracy (equal to 4/3 here; the rotational symmetry for O_2 is 2, TS1 has a mirror image, and the electronic degeneracy contribution is 1/3). h is Planck's constant. $G(E,J)_{\text{TS1}}$ is the sum of quantum states for TS1 at each pair of energy (E) and angular momentum (J). $\rho(E,J)_{\text{Re}}$ is the density of states of the reactants CH_3OO and O_2; $\rho(E,J)_{\text{Re}}$ is calculated as a convolution of the density of states for CH_3OO and O_2 by assuming that CH_3OO and O_2 can exchange internal energies freely. Therefore, $\rho(E,J)_{\text{Re}}$ can be expressed as

$$\rho(E,J)_{\text{Re}} = \int_0^E \rho(E_X,J)_{CH_3OO} \times \rho(E - E_X,J)_{O_2}\, dE_X \tag{5}$$

The SCTST code from the freely available MultiWell program suite[38−40] is used to compute the sum of vibrational states for TS1, while the ADENSUM code[41] is used to obtain the density of vibrational states for CH_3OO and O_2. These calculations are performed using a grain size of 10 cm^{-1} and a ceiling energy of 5 × 10^4 cm^{-1}. The barrier height and rovibrational parameters obtained from the high-level quantum chemical calculations in the previous section are used as input data and can be found in the Supporting Information.

Note that microcanonical rate constants $k(E,J)$ calculated using eq 4 include all vibrational, rotational, and electronic

dx.doi.org/10.1021/jp510554g | J. Phys. Chem. A XXXX, XXX, XXX−XXX

degrees of freedom, but not translational degrees of freedom, so they have units of inverse of second (1/s). The translational degrees of freedom are assumed to be separable and can then be included in computing thermal rate constants in eq 6:

$$k(T) = \frac{Q(T)^{TS}_{trans}}{Q(T)^{O_2}_{trans} \times Q(T)^{CH_3OO}_{trans}} \times \sum_{J=0}^{\infty} \int_0^{\infty} k(E, J) \times F(E, J)\, dE \tag{6}$$

where $Q(T)_{trans}$ is the translational partition function. $F(E,J)$ is the internal energy and angular momentum distribution function of the initial reactants, $CH_3OO^* + O_2$. $F(E,J)$ can be constructed using a two-dimensional master equation technique if reaction conditions of temperature and pressure are known a priori. Unfortunately, this is not the case in the discharge experiment. In the thermalized equilibrium condition, $F(E,J)$ is computed using the Boltzmann thermal distribution:

$$F(E, J) = \frac{(2J + 1)\rho_{Re}(E, J) \exp\left(-\frac{E}{RT}\right)}{\sum_{J=0}^{\infty} \int_{E=0}^{\infty} (2J + 1)\rho_{Re}(E, J) \exp\left(-\frac{E}{RT}\right) dE} \tag{7}$$

Substituting eqs 4 and 7 into eq 6, we obtain

$$k(T) = \frac{\sigma}{h} \times \frac{Q(T)^{TS}_{trans}}{Q(T)^{O_2}_{trans} \times Q(T)^{CH_3OO}_{trans}} \times \frac{1}{Q(T)^{Re}_{rv}} \times \sum_{J=0}^{\infty} (2J + 1) \int_0^{\infty} G(E, J)_{TS1} \exp\left(-\frac{E}{RT}\right) dE \tag{8}$$

where $Q(T)^{Re}_{rv}$ is the rovibrational partition function of the reactants and is given by

$$Q(T)^{Re}_{rv} = \sum_{J=0}^{\infty} \int_{E=0}^{\infty} (2J + 1)\rho_{Re}(E, J) \exp\left(-\frac{E}{RT}\right) dE \tag{9}$$

The thermal rate constant in eq 8 has the same form as obtained in transition state theory and has units of cm^3 $molecule^{-1}$ s^{-1}. However, the discharge experiment is a highly nonequilibrium system, so we feel it would be inappropriate to base our analysis on thermal rate constants. Rather, we use the microcanonical formalism that is energy-dependent and perhaps can be used more meaningfully in the present context.

Microcanonical rate constants, $k(E,J = 0)$, for the $CH_3OO + O_2 \rightarrow CH_2{=}O{-}O + HO_2$ reaction step are calculated as a function of internal energy relative to the asymptotic energy level of the initial reactants, $CH_3 + 2O_2$. The calculated results plotted in Figure 2 show that $k(E,J = 0)$ increases sharply when energy increases, for example from about 4×10^5 s^{-1} at the asymptotic level to ca. 1×10^{10} s^{-1} at TS1. Significantly, even at 2 kcal/mol below the asymptotic level, the reaction rate still remains appreciable, about 10^4 s^{-1}. Note that this regime is classically forbidden, thus quantum mechanical tunneling controls the reaction rate. Nascent Criegee, once formed, *must* be cold in this regime and can be detected. It should be mentioned that the pressure in the supersonic expansion (after passing through the discharge nozzle) is very low, so the collision frequency of energized CH_3OO with the buffer gas is estimated to be on the order of 10 s^{-1}, which obviously cannot compete with the formation rate of Criegee. Of course, warmer Criegee could also be stabilized by collisions in the discharge nozzle prior to the ultimately collision-free conditions in the supersonic expansion. However, in the discharge experiments[10]

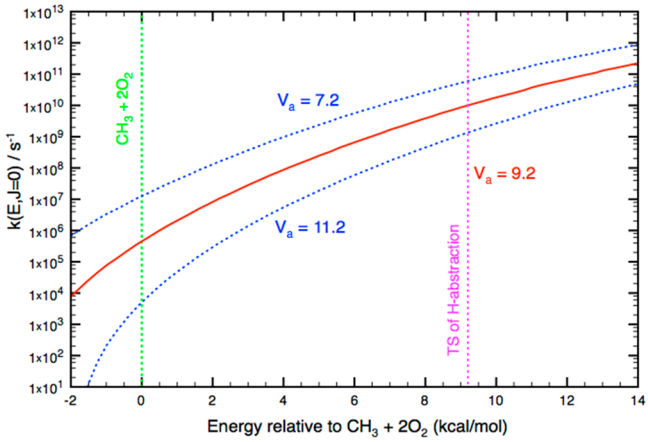

Figure 2. Microcanonical rate constant for forming the simplest Criegee intermediate in the CH_4/O_2 electric discharge experiment.

we do not see evidence for vibrationally hot CH_3OO, which will be required to yield vibrationally hot Criegee.

In computing $k(E,J)$, all vibrations were assumed to be coupled and anharmonic vibrational constants were computed using second-order vibration perturbation theory (VPT2). It is well-known that the VPT2 approach works well for small amplitude motions, but can fail for large amplitude motions such as hindered internal rotations in a molecule. In the H-abstraction transition structure TS1, there are two low vibrational frequencies that are 38 and 99 cm^{-1}. The former corresponds to the torsional motion of the OO− and OOC− groups around the C−O axis in TS1, while the latter is a complex bending motion. Both these vibrations have small anharmonic vibration constants (see the Supporting Information), thus they couple rather weakly with the remaining vibrations. Therefore, it is a good approximation to assume that they can be separated from the other vibrations. Here, the latter motion (ω = 99 cm^{-1}) is keep as a coupled vibration as before, while we separated the former vibration (38 cm^{-1}) from the remaining vibrations and treated it approximately as a 1D-hindered internal rotor. This rotor has a reduced moment of inertia of 20.604 amu·Å^2 and a torsional barrier height of 1775 cm^{-1}. However, the way that this very low-frequency mode is treated ultimately has only small effects on the kinetics. Such a separation causes an increase of the barrier by only 3 cm^{-1}. The cumulative reaction probability via TS1 is then recomputed and used to compare with the previously calculated results where it was assumed all vibrations are coupled. In the energy range in consideration, the difference between two models is found to be a factor of about 2 (see Figure S4 in the Supporting Information). Such a difference is much smaller than that caused by a possible error from the calculated barrier (see below).

It should be emphasized that tunneling through the barrier mainly produces cool Criegee. So, the required energy for this process is close to the energy level at TS1. In this energy region, the harmonic model is a good approximation, even when it is applied to a hindered internal rotor.

It is important to perform a sensitivity analysis to evaluate the accuracy expected of the calculated microcanonical rate constants. There are a number of factors that can affect the calculated $k(E,J = 0)$ values, which include barrier height, magnitude of the imaginary (barrier) frequency, rovibrational parameters, anharmonic constants, and hindered internal rotor

dx.doi.org/10.1021/jp510554g | J. Phys. Chem. A XXXX, XXX, XXX−XXX

effects. Of these, the barrier height with a likely error bar of about ±2 kcal/mol for TS1 is almost certain the dominant one. In contrast, other parameters are expected to have much smaller effects (e.g., less than a factor of 2). To proceed with the sensitivity analysis, we shifted the position of TS1 up and down by 2 kcal/mol and then recomputed $k(E,J)$, the results of which are also displayed in Figure 2. As expected, the rate constant increases or decreases corresponding to the drop or increase of the barrier. The change of rate becomes very important at low energies: for example, changing the activation energy alters $k(E)$ by 2 orders of magnitude at the energy level of $CH_3 + O_2$, but only by about a factor of 10 at the energy of the TS. Overall, within the estimated error bar of 2 kcal/mol for the calculated barrier, the microcanonical tunneling formation rates for cool Criegee still remain fast, even at the asymptotic level (see Figure 2).

So, we conclude that tunneling can plausibly lead to formation of cold Criegee, which does not have a sufficient energy to proceed to dioxirane (or to formic acid). This cold Criegee would be trapped in a well (that has a barrier height of about 19 kcal/mol) and becomes detectable as observed in our discharge experiment. The lifetime of Criegee at room temperature is estimated using SCTST to be a couple of seconds. For these reasons, we cannot rule out that a very small fraction of hot Criegee could be stabilized in the discharge nozzle source by collisions with the buffer gas.

To study the possible role of quantum mechanical tunneling in the formation of cold Criegee, we replaced CH_4 by its deuterated counterpart CD_4 and repeated the CD_4/O_2 discharge experiment under nearly identical conditions. Surprisingly, cold CD_2OO Criegee is also produced and detected. For this reason, we computed microcanonical rate constants as a function of internal energy relative to the asymptotic level of CD_3 plus O_2 and the $k(E)$ results are plotted in Figure 3. In addition, the formation rate of CH_2OO

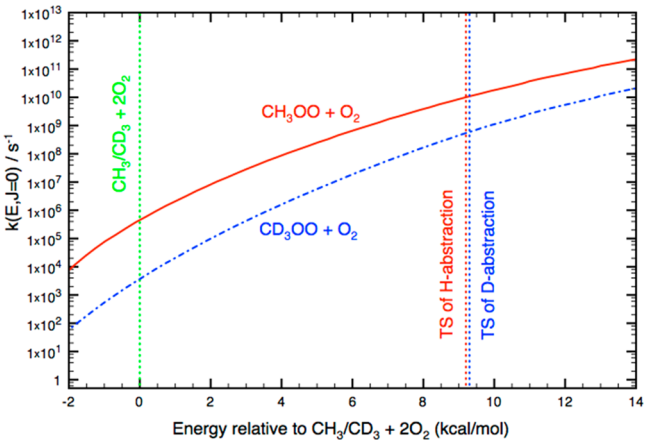

Figure 3. Microcanonical rate constants for forming the simplest Criegee intermediates in the CH_4 and CD_4/O_2 electric discharge experiments.

is also included for a direct comparison. Figure 3 shows that—like the formation rate of the normal isotopic species—the rate for CD_2OO increases significantly when energy increases. However, the CD_2OO rate is much slower than CH_2OO rate (by one to 2 orders of magnitude) depending on internal energy due to inhibition of tunneling by the higher mass of the deuterium atom. For example, the kinetic isotopic effect $KIE(CH_2OO/CD_2OO)$ is about 10 at TS, but becomes about 100 at the lower-energy asymptotic level of the initial reactants. Although the formation rate of CD_2OO is much slower than CH_2OO, it is still fast enough (from 4×10^3 to 6×10^8 s^{-1}) that cold Criegee can be produced and detected at these energies. Consequently, quantum mechanical tunneling also appears to be a viable formation route even for CD_2OO.

Our recent experimental results[10] showed a relative correlation between the formation of CH_2OO Criegee intermediate and the presence of CH_3OO. The formation of Criegee from either the self-reaction of CH_3OO radicals or the reaction of CH_3OO with HO_2 is excluded, according to both experimental and theoretical results reported for these reactions earlier.[42−45] In addition, we investigated possible alterative mechanism and associated kinetics for reactions of H atom with CH_3OO (see Figure S1) and of OH radical with CH_3OO (see Figure S2a,b). We found that the formation fraction of Criegee intermediate is negligible in these reaction channels (see the Supporting Information). Furthermore, there is no evidence from both experiment[46−50] and theory[51] for the formation of cool Criegee from the reaction of triplet CH_2 with triplet O_2. The association of CH_2 with O_2 leads to the formation of vibrationally excited adduct, CH_2OO^*, which has an internal energy of ca. 67 kcal/mol.[23−26] Hot CH_2OO^* will rapidly isomerize to dioxirane after overcoming a barrier of 19 kcal/mol. So, it cannot survive long enough for detection.

■ ASSOCIATED CONTENT

Supporting Information

Optimized geometries, rovibrational parameters, anharmonic constants, thermal rate constants, and energies for various species in the reaction of $2O_2$ with CH_3/CD_3 are given. In addition, the reaction mechanisms of H + CH_3OO and HO + CH_3OO are presented. This material is available free of charge via the Internet at http://pubs.acs.org.

■ AUTHOR INFORMATION

Corresponding Author

*E-mail: jfstanton@mail.utexas.edu.

Notes

The authors declare no competing financial interest.

■ ACKNOWLEDGMENTS

J.F.S. and T.L.N. are supported by the Robert A. Welch Foundation (Grant F-1283). This material is based on the work supported by the U.S. Department of Energy, Office of Basic Energy Sciences under Award Number DE-FG02-07ER15884. M.C.M. is supported by NSF Grant No. CHE-1058063.

■ REFERENCES

(1) Criegee, R.; Wenner, G. Die Ozonisierung Des 9, 10-Oktalins. *Chem. Ber.* **1949**, *564*, 9−15.
(2) Criegee, R. Mechanism of Ozonolysis. *Angew. Chem., Int. Ed. Engl.* **1975**, *14*, 745−752.
(3) Neeb, P.; Horie, O.; Moorgat, G. K. The Ethene-Ozone Reaction in the Gas Phase. *Chem. Phys. Lett.* **1998**, *102*, 6778−6785.
(4) Alam, M. S.; Bloss, W. J.; et al. Total Radicals Yields from Tropospheric Ethene Ozonolysis. *Phys. Chem. Chem. Phys.* **2011**, *13*, 11002−11015.
(5) Taatjes, C. A.; Meloni, G.; Selby, T. M.; Trevitt, A. J.; Osborn, D. L.; Percival, C. J.; Shallcross, D. E. Direct Observation of the Gas-Phase Criegee Intermediate (CH_2OO). *J. Am. Chem. Soc.* **2008**, *130*, 11883−11885.

(6) Welz, O.; Savee, J. D.; Osborn, D. L.; Vasu, S. S.; Percival, C. J.; Shallcross, D. E.; Taatjes, C. A. Direct Kinetic Measurements of Criegee Intermediate (CH_2O) Formed by Reaction of CH_2I with O_2. *Science* **2012**, *335*, 204−207.
(7) Su, Y. T.; Huang, Y. H.; Witek, H. A.; Lee, Y. L. Infrared Absorption Spectrum of the Simplest Criegee Intermediate CH_2OO. *Science* **2013**, *340*, 174−176.
(8) Nakajima, M.; Endo, Y. Communication: Determination of the molecular structure of the simplest Criegee intermediate CH_2OO. *J. Chem. Phys.* **2013**, *139*, 101103.
(9) Beames, J. M.; Liu, F.; Lu, L.; Lester, M. I. Ultraviolet Spectrum and Photochemistry of the Simplest Criegee Intermediate CH_2OO. *J. Am. Chem. Soc.* **2012**, *134*, 20045−20048.
(10) McCarthy, M. C.; Cheng, L.; Crabtree, K. N.; Martinez, O., Jr; Nguyen, T. L.; Womack, C. C.; Stanton, J. F. The Simplest Criegee Intermediate ($H_2C{=}O{-}O$): Isotopic Spectroscopy, Equilibrium Structure, and Possible Formation from Atmospheric Lightning. *J. Phys. Chem. Lett.* **2013**, *23*, 4133−4139.
(11) Christian, H.; Latham, J. Satellite Measurements of Global Lightning. *Quarterly J. R. Met. Soc.* **1998**, *124*, 1771−1773.
(12) Christian, H. J.; Blakeslee, R. J.; Boccippio, D. J.; Boeck, W. L.; Buechler, D. E.; Driscoll, K. T.; Goodman, S. J.; Hall, J. M.; Koshak, W. J.; Mach, D. M.; Stewart, M. F. Global Frequency and Distribution of Lightning as Observed from Space by the Optical Transient Detector. *J. Geophys. Res.* **2003**, *108*, ACL 4-1−ACL 4-15 DOI: 10.1029/2002JD002347.
(13) Tajti, A.; Szalay, P. G.; Csaszar, A. G.; Kallay, M.; Gauss, J.; Valeev, E. F.; Flowers, B. A.; Vazquez, J.; Stanton, J. F. HEAT: High Accuracy Extrapolated Ab Initio Thermochemistry. *J. Chem. Phys.* **2004**, *121*, 11599−11613.
(14) Bomble, Y. J.; Vazquez, J.; Kallay, M.; Michauk, C.; Szalay, P. G.; Csaszar, A. G.; Gauss, J.; Stanton, J. F. High-Accuracy Extrapolated Ab Initio Thermochemistry. II. Minor Improvements to the Protocol and a Vital Simplification. *J. Chem. Phys.* **2006**, *125*, 064108−8.
(15) Harding, M. E.; Vazquez, J.; Ruscic, B.; Wilson, A. K.; Gauss, J.; Stanton, J. F. High-Accuracy Extrapolated Ab Initio Thermochemistry. III. Additional Improvements and Overview. *J. Chem. Phys.* **2008**, *128*, 114111−15.
(16) Almlof, J.; Taylor, P. R. General Constraction of Gaussian-Basis Sets. 1. Atomic Natural Orbitals for 1st-Row and 2nd-Row Atoms. *J. Chem. Phys.* **1987**, *86*, 4070−4077.
(17) Almlof, J.; Taylor, P. R. General Constraction of Gaussian-Basis Sets. 2. Atomic Natural Orbitals and the Calculation of Atomic and Molecular-Properties. *J. Chem. Phys.* **1990**, *92*, 551−560.
(18) McCaslin, L. M.; Stanton, J. F. Calculation of Fundamental Frequencies for Small Polyatomic Molecules: A Comparison of Correlation-Consistent and Atomic Natural Orbital Basis Sets. *Mol. Phys.* **2013**, *111*, 1492−1496.
(19) Mills, I. M. Vibration−Rotation Structure in Asymmetric- and Symmetric-Top Molecules. In *Molecular Spectroscopy: Modern Research*; Rao, K. N.; Mathews, C. W., Eds.; Academic Press: New York, 1972; Vol. *1*, p 115.
(20) Dunning, T. H., Jr. Gaussian Basis Sets for Use in Correlated Molecular Calculations. I. The Atoms Boron through Neon and Hydrogen. *J. Chem. Phys.* **1989**, *90*, 1007−1023.
(21) Feller, D. Application of Systematic Sequences of Wave-Functions to the Water Dimer. *J. Chem. Phys.* **1992**, *96*, 6104−6114.
(22) Helgaker, T.; Klopper, W.; Koch, H.; Noga, J. Basis-Set Convergence of Correlated Calculations on Water. *J. Chem. Phys.* **1997**, *106*, 9639−9646.
(23) Ruscic, B.; Pinzon, R. E.; Morton, M. L.; von Laszevski, G.; Bittner, S. J.; Nijsure, S. G.; Amin, K. A.; Minkoff, M.; Wagner, A. F. Introduction to Active Thermochemical Tables: Several "Key" Enthalpies of Formation Revisited. *J. Phys. Chem. A* **2004**, *108*, 9979−9997.
(24) Ruscic, B.; Pinzon, R. E.; von Laszevski, G.; Kodeboyina, D.; Burcat, A.; Leahy, D.; Montoya, D.; Wagner, A. F. Active Thermochemical Tables: Thermochemistry for the 21st Century. *J. Phys. Conf. Ser.* **2005**, *16*, 561−570.
(25) Ruscic, B.; Pinzon, R. E.; Morton, M. L.; Srinivasan, N. K.; Su, M.-C.; Sutherland, J. W.; Michael, J. V. Active Thermochemical Tables: Accurate Enthalpy of Formation of Hydroperoxyl Radical, HO_2. *J. Phys. Chem. A* **2006**, *110*, 6592−6601.
(26) Ruscic, B. Updated Active Thermochemical Tables (ATcT) Values Based on ver. 1.110 of the Thermochemical Network (2012); available at http://atct.anl.gov.
(27) Stanton, J. F.; Gauss, J.; Harding, M. E.; Szalay, P. G.; Auer, A. A.; Bartlett, R. J.; et al. *CFOUR, a Quantum Chemical Program Package*, 2009 (available at http://www.cfour.de).
(28) MRCC, a Quantum Chemical Program Suite written by Kállay, M.; Rolik, Z.; Ladjánszki, I. ; Szegedy, L.; Ladóczki, B.; Csontos, J.; Kornis, B. See also Kállay, M.; Rolik, Z. *J. Chem. Phys.* **2011**, *135*, 104111 as well as http://www.mrcc.hu.
(29) Zhu, R.; Hsu, C.-C.; Lin, M. C. Ab initio study of the $CH_3 + O_2$ reaction: Kinetics, mechanism and product branching probabilities. *J. Chem. Phys.* **2001**, *115*, 195−203.
(30) Salter, E. A.; Sekino, H.; Bartlett, R. J. Property Evaluation and Orbital Relaxation in Coupled Cluster Methods. *J. Chem. Phys.* **1987**, *87*, 502−509.
(31) Gutbrod, R.; Schindler, R. N.; Kraka, E.; Cremer, D. Formation of OH Radicals in the Gas Phase Ozonelysis of Alkenes: The Unexpected Roles of Carbonyl Oxides. *Chem. Phys. Lett.* **1996**, *252*, 221−229.
(32) Olzmann, M.; Kraka, E.; Cremer, D.; Gutbrod, R.; Andersson, S. Energetics, Kinetics, and Product Distributions of the Reactions of Ozone with Ethene and 2,3-Dimethyl-2-butene. *J. Phys. Chem. A* **1997**, *101*, 9421−9429.
(33) Donahue, N. M.; Kroll, J. H.; Anderson, J. G.; Demerjian, K. L. Direct Observation of OH Production from the Ozonolysis of Olefins. *Geophys. Res. Lett.* **1998**, *25*, 59−62.
(34) *NIST Computational Chemistry Comparison and Benchmark Database*; NIST Standard Reference Database Number 101, Release 16a; Johnson R. D., III, Ed., August 2012; http://cccbdb.nist.gov/.
(35) Miller, W. H. Semi-Classical Theory for Non-Separable Systems:. Construction of "Good" Action-Angle Variables for Reaction Rate Constants. *Faraday Disc. Chem. Soc.* **1977**, *62*, 40−46.
(36) Miller, W. H.; Hernandez, R.; Handy, N. C.; Jayatilaka, D.; Willets, A. Ab Initio Calculation of Anharmonic Constants for a Transition-State, with Application to Semiclassical Transition-State Tunneling Probabilities. *Chem. Phys. Lett.* **1990**, *172*, 62−68.
(37) Hernandez, R.; Miller, W. H. Semi-Classical Transition State Theory. A New Perspective. *Chem. Phys. Lett.* **1993**, *214*, 129−136.
(38) Nguyen, T. L.; Stanton, J. F.; Barker, J. R. A Practical Implementation of Semi-Classical Transition State Theory for Polyatomics. *Chem. Phys. Lett.* **2010**, *499*, 9−15.
(39) Nguyen, T. L.; Stanton, J. F.; Barker, J. R. Ab Initio Reaction Rate Constants Computed Using Semiclassical Transition-State Theory: HO + H_2 = H_2O + H and Isotopologues. *J. Phys. Chem. A* **2011**, *115*, 5118−5126.
(40) Barker, J. R.; Ortiz, N. F.; Preses, J. M.; Lohr, L. L.; Maranzana, A.; Stimac, P. J.; Nguyen, T. L.; Kumar, T. J. D. *MultiWell Program Suite*; University of Michigan: Ann Arbor, MI, 2011 (http://aoss.engin.umich.edu/multiwell/).
(41) Nguyen, T. L.; Barker, J. R. Sums and Densities of Fully Coupled Anharmonic Vibrational States: A Comparison of Three Practical Methods. *J. Phys. Chem. A* **2010**, *114*, 3718−3730.
(42) Liang, Y. N.; Li, J.; Wang, Q. D.; Li, X. Y. Computational Study of the Reaction Mechanism of the Methylperoxy Self-Reaction. *J. Phys. Chem. A* **2011**, *115*, 13534−13541.
(43) Wang, B.; Hou, H. A Systematic Computational Study on the Reactions of HO_2 with RO_2: The $HO_2 + CH_3O_2(CD_3O_2)$ and $HO_2 + CH_2FO_2$ Reactions. *J. Phys. Chem. A* **2005**, *109*, 451−460.
(44) Raventos-Duran, M. T.; McGillen, M.; Hamer, P. D.; ShallCross, D. E. Kinetics of the $CH_3O_2 + HO_2$ Reaction: A Temperature and Pressure Dependence Study Using Chemical Ionization Mass Spectrometry. *Int. J. Chem. Kinet.* **2007**, *39*, 571−579.
(45) Orlando, J. J.; Tyndall, G. S. Laboratory Studies of organic Peroxy Radical Chemistry: An Overview with Emphasis on Recent

Issues of Atmospheric Significance. *Chem. Soc. Rev.* **2012**, *41*, 6294−6317.
(46) Alvarez, R. A.; Moore, C. B. Absolute Yields of CO, CO_2, and H_2CO from the Reaction $CH_2(X^3B_1) + O_2$ by IR Diode Laser Flash Kinetic Spectroscopy. *J. Phys. Chem.* **1994**, *98*, 174−183.
(47) Hancock, G.; Haverd, V. A Time-Resolved FTIR Emission Study of the Gas Phase Removal Process of $CH_2(X^3B_1)$ and $CH_2(a^1A_1)$ in Collisions with O_2. *Chem. Phys. Lett.* **2003**, *372*, 288−294.
(48) Blitz, M. A.; McKee, K. W.; Pilling, M. J.; Seakins, P. W. Evidence for the Dominance of Collision-Induced Intersystem Crossing in Collisions of $^1CH_2$ with O_2 and a Determination of the H Atom Yields from $^3CH_2 + O_2$ Using Time-Resolved Detection of H Formation by vuvLIF. *Chem. Phys. Lett.* **2003**, *372*, 295−299.
(49) Su, H.; Mao, W.; Kong, F. Reactions of $CH_2(X^3B_1)$ and $CH_2(a^1A_1)$ with O_2 Studied by Time-Resolved FTIR Spectroscopy. *Chem. Phys. Lett.* **2000**, *322*, 21−26.
(50) Lee, P. F.; Matsui, H.; Chen, W. Y.; Wang, N. S. Production of H and $O(^3P)$ Atoms in the Reaction of CH_2 with O_2. *J. Phys. Chem. A* **2012**, *116*, 9245−9254.
(51) Fang, D. C.; Fu, X. Y. CASSCF and CAS+1 + 2 Studies on the Potential Energy Surface and the Rate Constants for the Reactions between CH_2 and O_2. *J. Phys. Chem. A* **2002**, *106*, 2988−2993.

dx.doi.org/10.1021/jp510554g | *J. Phys. Chem. A* XXXX, XXX, XXX−XXX